*ICIC Express Letters*
Volume **16**, Number **12**, December **2022**
 ISSN 1881-803X
pp. **1259–1267**

# SIMULATION BASED MOTION PLANNING OF WMR UNDER LOCAL MINIMUM CONDITION USING IAPF ALGORITHM

Riky Dwi Puriyanto[1,2,*], Oyas Wahyunggoro[1] and Adha Imam Cahyadi[1]

[1]Department of Electrical and Information Engineering
Universitas Gadjah Mada
Bulaksumur, Yogyakarta 55281, Indonesia
{ oyas; adha.imam }@ugm.ac.id

[2]Department of Electrical Engineering
Universitas Ahmad Dahlan
Jl. Ringroad Selatan, Tamanan, Bantul, Yogyakarta 55191, Indonesia
*Corresponding author: rikydp@ee.uad.ac.id

Received December 2021; accepted March 2022

Abstract. *Autonomous robots have been developed in various applications to simplify human tasks. One of the platforms used is a wheeled mobile robot (WMR). The problem encountered in the implementation of autonomous WMR is navigation. In navigation, path planning is considered necessary in minimizing investment in development time and finance. One algorithm that is considered reliable and is still used today is the artificial potential field (APF) path planning algorithm. However, this algorithm has a shortcoming when it meets local minimum conditions. In this study, a potential field-based algorithm was developed by changing the shape of the potential repulsive field into a cone-shaped repulsive potential field. In addition, the Gompertz function is used as a switching function for two different conditions. The path planning algorithm is implemented on the WMR kinematics model. The test results show that the improved artificial potential field (IAPF) algorithm can produce a collision-free path under minimum local conditions. The local minimum forms used in the test are symmetrically aligned robot-obstacle-goal (SAROG), symmetric static object distribution (SSOD), and goal non-reachable due to obstacle nearby (GNRON). In addition, the nature of the obstacle used is static and dynamic. All test results show that the IAPF algorithm can work in static and dynamic conditions with the resulting $E_{rg}$ less than 1% and the average value of $D_{\min}$ is 2.22 m.*
**Keywords:** Potential field, Local minimum, Wheeled mobile robot, Gompertz function, SAROG, SSOD, GNRON

1. **Introduction.** Nowadays, autonomous mobile robots are becoming one of the exciting topics for researchers. Autonomous mobile robots are widely applied in many applications [1-3]. Wheeled mobile robot (WMR) is one type of mobile robot with advantages in mobility and flexibility. Human habits in using cars make this robot platform choose the kind of robot that moves on the ground. The problems faced in autonomous WMR are motion planning and control of the robot. Motion planning or path planning is used to plan the path traversed by the robot from the initial position to the goal position while avoiding obstacles in between. Motion control is used to adjust the robot's motion to move according to the planned path.

In completing the task, the kinematics of the WMR model is used to determine the expected motion by adjusting the motion of the actuator and estimating the state of motion of the WMR with the perceived degrees of freedom (DOF) at the same time. When the robot goes to the goal while avoiding collisions with obstacles, the kinematic model of WMR needs to be equipped with navigation capabilities [4]. WMR also must

DOI: 10.24507/icicel.16.12.1259

have navigational skills to complete the task properly. There are four basic components of navigation, which are perception, localization, mapping, and path planning [5]. Path planning is one of the main navigation components that a robot must have to avoid obstacles in the work environment [6-8]. A good path planning algorithm can reduce the time investment needed in robot development [9, 10].

One of the path planning algorithms that is considered reliable and is still used today is the artificial potential field (APF) [11]. However, this algorithm has a shortcoming where the robot can be trapped in minimum local conditions. The local minimum form faced by the APF algorithm is commonly referred to as goal non-reachable due to obstacle nearby (GNRON) [12], and symmetrically aligned robot-obstacle-goal (SAROG) [13]. The modification of the SAROG problem with two obstacles located symmetrically between the robot and the goal is called symmetric static object distribution (SSOD). These three local minimum forms are generally still being solved by researchers using APF-based path planning algorithms.

Based on existing research in recent years, the solutions to SSOD and SAROG problems can be grouped into 1) using virtual force [14-16], 2) changing the shape of the repulsive potential field generated by the obstacle [17], and 3) changing resultant force [8, 18]. Many researchers have also solved the GNRON problem [10, 14-22]. Currently, the solution to the GNRON problem which is considered robust is to multiply the repulsive potential field equation by the robot's distance to the target. This method results in a gradual decrease in the repulsive potential field around the target. This is considered to be able to solve the GNRON problem.

This research will solve the problems of SSOD, SAROG, and GNRON separately or in combination. The research contributions given are

- Changing the shape of the repulsive potential field based on the cone-shaped potential field and determining the repulsive gain value ($\eta$) based on the attractive gain value ($\xi$);
- Minimizing the use of switching functions (if-else) to avoid nested if-else using Gompertz function;
- Implementing the cone-based potential field algorithm on the WMR kinematic model.

This paper is structured as follows: Section 2 describes the basic concept of traditional APF (TAPF) path planning algorithm, Section 2 also introduces the proposed path planning algorithm approach and describes the experimental design which contains the design of the kinematic model and test parameters, Section 3 presents simulation and test results of the proposed methods, and finally, Section 4 summarizes the results.

## 2. **Method.**

### 2.1. **Basic concept of traditional artificial potential field (TAPF).**

The working principle of the TAPF path planning algorithm can be seen in Figure 1. The robot moves in an environment close to the goal, which produces an attractive potential force while moving away from the obstacle, which generates a repulsive potential force. The red line represents the obstacle's repulsive force, while the green line is the attractive force generated by the goal, which functions to draw the robot closer to the goal. The black line represents the path of the robot makes from the starting position to the goal while avoiding the obstacle in between.

The coordinates of the robot in an environment are defined as $q = (x, y)$. The TAPF algorithm generates a path that can be passed by the robot based on the distance parameter between robot-goal ($S_{rg}$), obstacle-goal ($S_{or}$), and the distance of the robot is affected by the repulsive potential field ($r$). According to the researcher [11], the attractive and

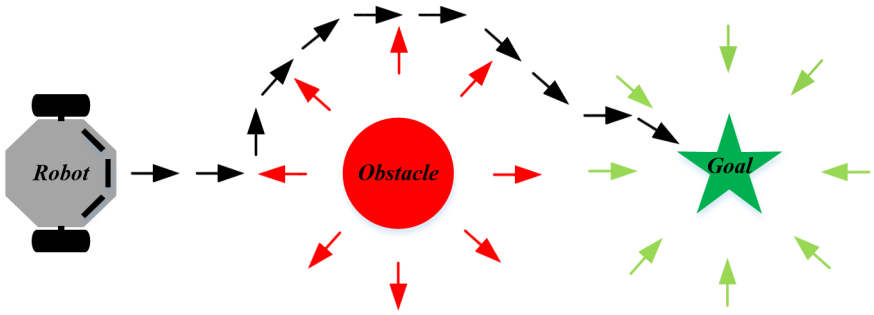


FIGURE 1. The working principle of the TAPF algorithm

repulsive potential field equations can be seen in (1) and (2).

$$U_{att}(q) = \frac{1}{2}\xi S_{rg}^2 \tag{1}$$

$$U_{rep.i}(q) = \begin{cases} \frac{1}{2}\eta\left(\frac{1}{S_{or}} - \frac{1}{r}\right)^2 & \text{if } S_{or} \leq r \\ 0 & \text{if } S_{or} > r \end{cases} \tag{2}$$

Based on (1) and (2), the total value of the potential field generated by Khatib's TAPF can be seen in (3). Parameter $k$ shows the number of obstacles in the environment.

$$U_{TAPF}(q) = U_{att}(q) + \sum_{i=1}^{n} U_{rep.i}(q) \tag{3}$$

The parameters $\xi$ and $\eta$ in Equations (1) and (2) are the attractive gain and the repulsive gain, respectively, whereas $S_{rg} = \|q_r - q_{goal}\|$ and $S_{or} = \|q_{obs} - q_r\|$ are the Euclidean distances between robot-goal and obstacle-robot. According to (2), the value of the repulsive potential field will affect the robot when $S_{or} \leq r$, while in other conditions, the repulsive potential field's value is zero.

The goal of path planning on the robot is to go to goal coordinates. The negative gradient of the attractive and repulsive potential fields shows the direction of the force generated by the TAPF algorithm towards the goal. The negative gradient $(-\nabla U_{TAPF}(q))$ of the TAPF function is needed to reach the goal position. The negative gradient indicates decreasing energy from the initial position to the goal position. The minimum energy is in the goal position.

The shortcoming of the TAPF algorithm is that robot can be trapped in local minimum condition. Local minimum problems can occur in several forms, as shown in Figure 2. The problem of symmetrically aligned robot-obstacle-goal (SAROG) in Figure 2(a) is caused by the position of the robot, which is one line with the obstacle and goal. The next problem is symmetric static object distribution (SSOD). According to Figure 2(b), this problem occurs when there is more than one obstacle that is symmetrically located between the robot and the obstacle. In this condition, the resultant repulsive force of obstacles received by the robot is proportional to the attractive force received by the robot from the goal. Another form of local minimum is a goal non-reachable due to obstacle nearby (GNRON). According to Figure 2(c), GNRON occurs when the obstacle is located very close to the $(S_{og} \leq r)$, where $S_{og} = \|q_{obs} - q_{goal}\|$. In this condition, the global minimum position will change due to the influence of the repulsive potential force near the goal.

2.2. **Improved artificial potential field (IAPF).** In this study, the attractive potential field used is following Equation (1), while the repulsive potential field is designed to

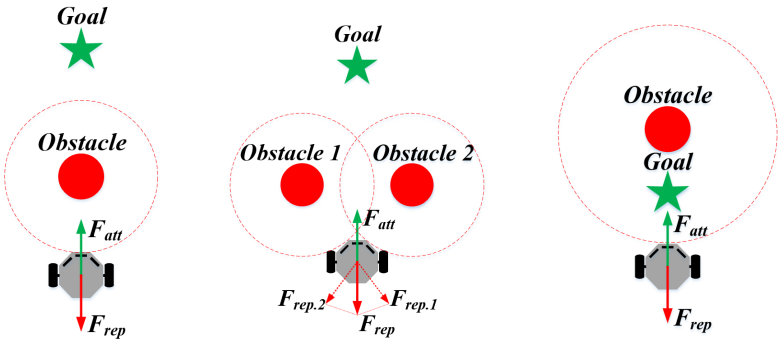


(a) SAROG (b) SSOD (c) GNRON

FIGURE 2. Local minimum condition

be felt in the range of $S_{or} \leq r$. The peak value of the repulsive potential field must be greater than the surrounding area to avoid collisions with obstacles. Cone-shape repulsive potential fields can be used to represent this strategy. The use of cone-shaped potential fields makes it easier for researchers to determine the value of the repulsive gain used. In this form, the value of $\eta$ is used to determine the amplitude of the repulsive potential field. Therefore, the relationship between attractive gain ($\xi$) and repulsive gain ($\eta$) can be determined easily. The if-else branching function, which represents the condition affected by the repulsive potential field, is replaced with the Gompertz function. This aims to minimize nested if-else in the path planning algorithm.

In this research, the SAROG problem is solved by generating a deflection function between the robot and the obstacle. A more complex problem than SAROG is SSOD. The SSOD problem is solved by adding an artificial repulsive force based on the distance of two adjacent obstacles. This force is generated by an artificial obstacle generated by two adjacent obstacles ($\|q_{obs.1} - q_{obs.2}\| < 2r$). The GNRON problem is solved by adding distance of robot to goal ($S^n_{rg}$) parameter as a multiplier in repulsive potential field equation. Based on the previously described strategy, the proposed repulsive potential field equation can be seen in (4).

$$U_{rep}(q) = e^{-e^{0.1\eta(S_{or}-r)}}(\eta - S_{or})S^n_{rg} + \psi + U_{ao}(q) \tag{4}$$

where $\eta = 10\xi$, $\psi$ is the solution to the SAROG problem, and $U_{ao}(q)$ is the solution to the SSOD problem. $\psi$ is the function of turning the robot between the robot and the obstacle. The $\psi$ equation can be seen in (5).

$$\psi = \left(\frac{1}{1+e^{y-y_o}} + \frac{1}{1+e^{x-x_o}}\right) \tag{5}$$

Based on Equation (5), the maximum potential field value generated at $y < y_o$ and $x < x_o$ is 2. Other conditions indicate that the potential field value near the target is 0.

$U_{ao}(q)$ is an artificial potential repulsive field generated by two adjacent obstacles. This problem is rarely found because researchers generally provide more distance between obstacles. However, the robot can experience a deadlock in this condition when it is at the junction between 2 obstacles. The artificial obstacle coordinates are given according to Equation (6).

$$x_{ao} = \frac{x_{o.1} + x_{o.2}}{2}; \quad y_{ao} = \frac{y_{o.1} + y_{o.2}}{2} \tag{6}$$

This obstacle can produce the same repulsive potential field as the real obstacle according to Equation (7).

$$U_{ao}(q) = \begin{cases} e^{-e^{0.1\eta(S_{aor}-r)}}(\eta - S_{aor})S^n_{rg} + \left(\frac{1}{1+e^{y-y_{ao}}} + \frac{1}{1+e^{x-x_{ao}}}\right) & \text{if } D \leq 2r \\ 0 & \text{if } D > 2r \end{cases} \tag{7}$$

where $S_{aor} = \left\| \frac{q_{ao}-q}{2r} \right\|$ and $D = \|q_{obs.1} - q_{obs.2}\|$. The total potential field equation proposed to solve the local minimum problem can be seen in (8)

$$\begin{gathered} U_{IAPF}(q) = U_{att}(q) + U_{rep}(q) \\ U_{IAPF}(q) = \frac{1}{2}\xi S_{rg}^2 + e^{-e^{0.1\eta(S_{or}-r)}}(\eta - S_{or})S_{rg}^n + U_{ao}(q_{ao}) + \psi \end{gathered} \tag{8}$$

The potential field equation is a scalar, while the negative gradient of the potential field is the vector [23]. The negative gradient of the IAPF function is used to minimize the available energy. Therefore, the robot can move from high potential field (initial position) to low potential field (goal position). The total force at a given point is a function that defines the vector force field. The total force represents the force received by the robot due to the pulling force from the target and the repulsion force generated by the obstacle. The total force value can also represent the resultant force received by the robot. The negative gradient of the function (8) can be seen in Equation (9).

$$\begin{aligned} F_x(q) &= -\frac{dU_{IAPF}(q)}{dx} \\ F_y(q) &= -\frac{dU_{IAPF}(q)}{dy} \end{aligned} \tag{9}$$

The resultant force represents the coordinates of the robot to reach the target. Therefore, the robot must perform the movement using the angle ($\delta$) formed by the resultant force. The value of the robot's heading angle is determined by equation $\delta = atan2(F_y(q), F_x(q))$.

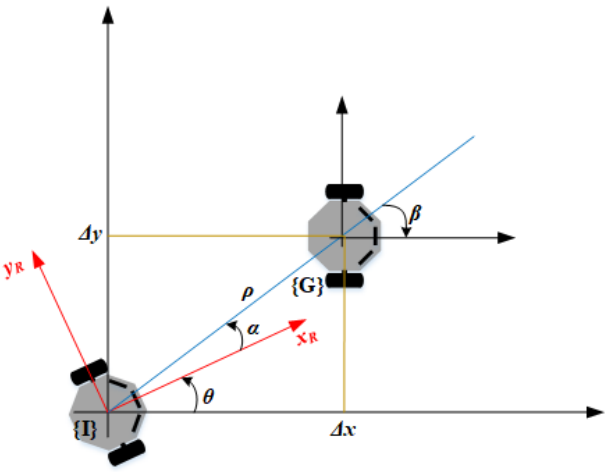


FIGURE 3. Kinematics model of WMR

2.3. **Kinematic model of WMR.** In this study, the path planning algorithm will be implemented in the kinematics of mobile robots according to Equation (10)

$$\begin{aligned} \dot{x} &= v\cos\theta \\ \dot{y} &= v\sin\theta \\ \dot{\theta} &= \omega \end{aligned} \tag{10}$$

Based on Figure 3, robot position can be represented in polar coordinates involving distance difference ($\rho > 0$) according to Equation (22) and change variable in (23).

$$\begin{aligned} \rho &= \sqrt{\Delta x^2 + \Delta y^2} \\ \alpha &= \tan^{-1}\left(\frac{F_y(q)}{F_x(q)}\right) - \theta \\ \beta &= -\theta - \alpha \end{aligned} \tag{11}$$

where $\Delta x = (x_i - x_g)$ and $\Delta y = (y_i - y_g)$. Therefore, when the value of $\alpha$ is located between $-\frac{\pi}{2}$ and $\frac{\pi}{2}$, the kinematics equation based on polar coordinates can be seen in (12). The negative gradient of the APF algorithm produces values and directions that can be used to determine the equilibrium point. The parameter of $F_x(q)$ and $F_y(q)$ is a tangent line of IAPF function.

$$\begin{aligned} \dot{\rho} &= -v\cos\alpha \\ \dot{\alpha} &= -\omega + \frac{v\sin\theta}{\rho} \\ \dot{\beta} &= -\frac{v\sin\theta}{\rho} \end{aligned} \tag{12}$$

The equations of linear velocity ($v$) and angular velocity ($\omega$) that are used to make the robot reach the goal as the origin can be seen in (13) and (14).

$$v = k_\rho \rho\cos\alpha; \quad k_\rho > 0 \tag{13}$$

$$\omega = k_\alpha \alpha; \quad k_\alpha > 0 \tag{14}$$

3. **Result and Discussion.** In order to evaluate the performance of the path planning algorithm, the environment around the robot is designed to have minimum local problems separately or in combination. Table 1 shows the coordinates of the initial, obstacle, and goal positions.

Table 1. Environmental setup

| Environment | Coordinate | | | Problem |
|---|---|---|---|---|
| | Initial $(x_i, y_i)$ | Obstacle $(x_o, y_o)$ | Goal $(x_g, y_g)$ | |
| EN1 | $(0, 5)$ | $(5, 5)$ | $(10, 5)$ | SAROG |
| EN2 | $(0, 5)$ | $(8.5, 5.5)$ | $(10, 5)$ | GNRON |
| EN3 | $(0, 5)$ | $(5, 6.5)$; $(5, 3.5)$ | $(10, 5)$ | SSOD |
| EN4 | $(0, 5)$ | $(8.5, 5)$ | $(10, 5)$ | SAROG+GNRON |
| EN5 | $(0, 5)$ | $(5\text{-}0.001t, 5)$ | $(10, 5)$ | Dynamic SAROG |
| EN6 | $(0, 5)$ | $(7\text{-}0.001t, 6.5)$; $(7\text{-}0.001t, 3.5)$ | $(10, 5)$ | Dynamic SSOD |

Some of the parameters used to evaluate the performance of the path planning algorithm in testing include the robots mileage ($D_{trav}$) and the error position of the robot against the goal ($E_{rg}$) according to (15).

$$\begin{aligned} D_{trav} &= \sum_{k=1}^{N} \|q_k - q_{k-1}\| \text{ meter} \\ E_{rg} &= \|q_{end} - q_g\| \text{ meter} \\ D_{\min} &= \|q_{obs} - q\| \text{ meter} \end{aligned} \tag{15}$$

where $q_k$, $q_{k-1}$, and $q_{end}$ are the current position, previous position, and the robot's final position, respectively.

Based on the test results in Figures 4(a)-4(f), implementing the TAPF algorithm on the WMR kinematic model can only deal with the static SAROG problem. The IAPF algorithm successfully solves all static and dynamic problems. The error to the goal ($E_{rg}$) of the IAPF algorithm on all test results is less than 1%. Robots with the IAPF algorithm can achieve goals and successfully avoid obstacles in between. Summary of the test results in all of the environments can be seen in Table 2.

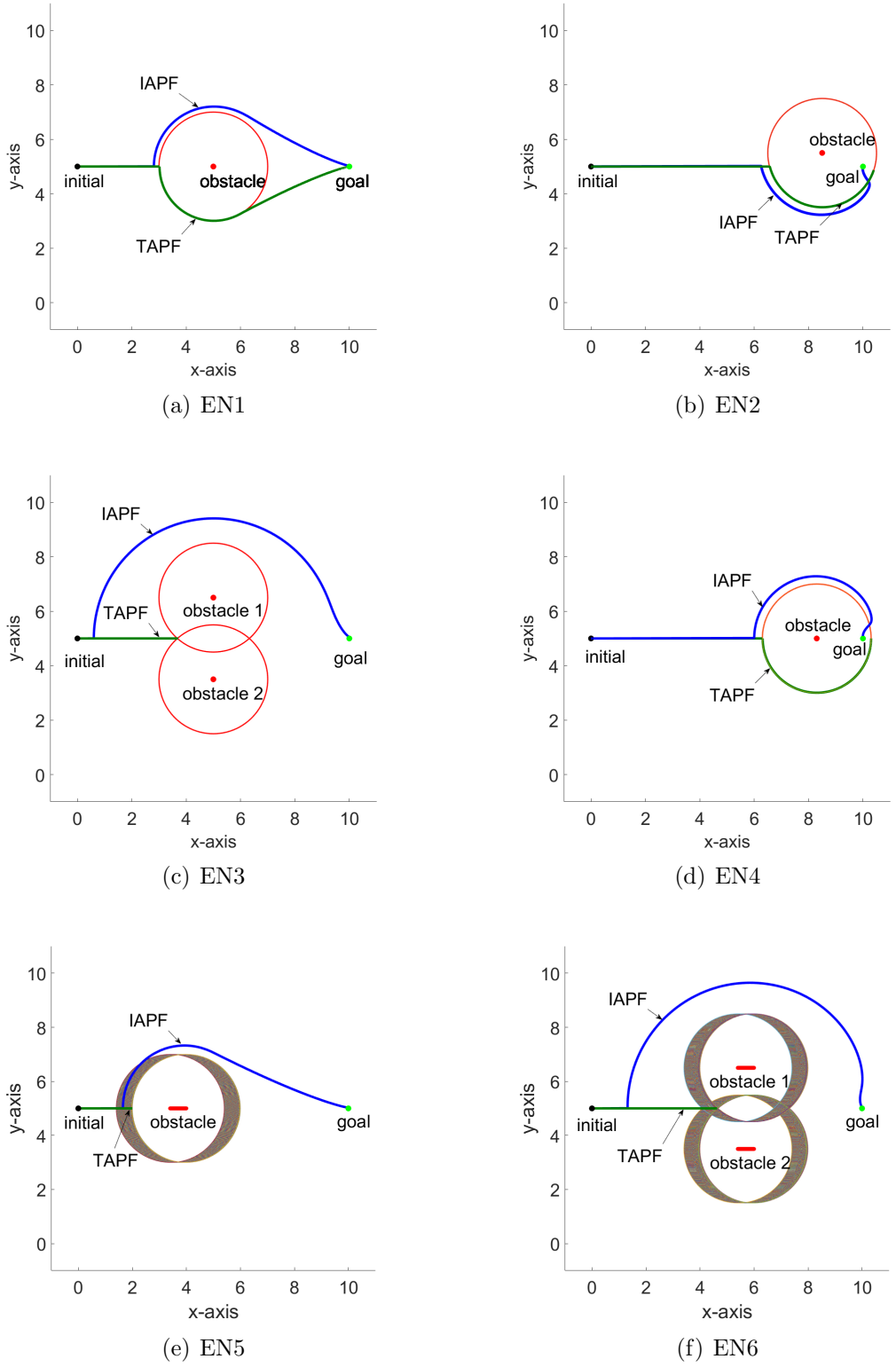


(a) EN1 (b) EN2

(c) EN3 (d) EN4

(e) EN5 (f) EN6

FIGURE 4. Trajectory of TAPF and IAPF in each environment

Based on Table 2, the TAPF algorithm has an average minimum distance value ($D_{\min}$) of 2 m. In EN2-EN6, the TAPF algorithm fails to reach the target and stops at $S_{or} = 2$ m. In the IAPF algorithm, the lowest $D_{\min}$ is found in EN2 and EN4 because they face the GNRON problem. In the SSOD (EN3) problem, the resulting $D_{\min}$ value is 2.91 m. The IAPF algorithm produces a $D_{\min}$ of 2.19 m in the SAROG problem. The average $D_{\min}$ value generated by the IAPF algorithm is 2.22 m.

TABLE 2. Summary of test results

| Algorithm | Criteria | Environment | | | | | |
|---|---|---|---|---|---|---|---|
| | | EN1 | EN2 | EN3 | EN4 | EN5 | EN6 |
| TAPF | $GR$ | Y | N | N | N | N | N |
| | $D_{trav}$ (m) | 13.7 | 10.7 | 3.7 | 14.2 | 2.0 | 1.6 |
| | $E_{rg}$ (m) | 0.09 | 0.42 | 6.30 | 0.30 | 8.00 | 5.37 |
| | $D_{\min}$ (m) | 2.00 | 2.00 | 2.00 | 2.00 | 2.00 | 2.00 |
| IAPF | $GR$ | Y | Y | Y | Y | Y | Y |
| | $D_{trav}$ (m) | 11.69 | 12.23 | 14.62 | 13.50 | 11.61 | 15.21 |
| | $E_{rg}$ (m) | 0.09 | 0.08 | 0.06 | 0.09 | 0.04 | 0.06 |
| | $D_{\min}$ (m) | 2.19 | 1.60 | 2.91 | 1.53 | 2.19 | 2.91 |

$GR$ = goal reachability

4. **Conclusions.** This paper introduces the IAPF algorithm, which is developing an APF-based path planning algorithm that is implemented on the kinematic model of wheeled mobile robot (WMR). The simulation results show that the IAPF algorithm that uses cone-shape based and additional function ($\psi$) in the repulsive potential field equation has succeeded in influencing the angle changes produced by the robot before it reaches the local minimum. The developed algorithm can generate collision-free paths in a static environment and a dynamic environment. Based on the test results, the robot can go to the goal with an error to the goal ($E_{rg}$) less than 1% and the average value of $D_{\min}$ is 2.22 m. This research contains limitations and can still be developed for further study by implementing a path planning algorithm in real robot implementation. Implementation in real conditions can verify the success of the IAPF path planning algorithm.

## REFERENCES


[1] H. Li and A. V. Savkin, An algorithm for safe navigation of mobile robots by a sensor network in dynamic cluttered industrial environments, *Robotics and Computer-Integrated Manufacturing*, vol.54, pp.65-82, 2018.

[2] F. Arvin, J. Espinosa, B. Bird, A. West, S. Watson and B. Lennox, Mona: An affordable open-source mobile robot for education and research, *Journal of Intelligent Robotic Systems*, vol.4, no.3, pp.761-775, 2019.

[3] Q. Qiu, Z. Fan, Z. Meng, Q. Zhang, Y. Cong, B. Li, N. Wang and C. Zhao, Extended Ackerman Steering Principle for the coordinated movement control of a four wheel rive agricultural mobile robot, *Computers and Electronics in Agriculture*, vol.152, pp.40-50, 2018.

[4] Z. Han, S. Yuan, X. Li and J. Zhou, Enhanced closed-loop systematic kinematics analysis of wheeled mobile robots, *International Journal of Advanced Robotic Systems*, vol.16, no.4, 2019.

[5] B. Patle, G. L. Babu, A. Pandey, D. Parhi and A. Jagadeesh, A review: On path planning strategies for navigation of mobile robot, *Defence Technology*, vol.15, no.4, pp.582-606, 2019.

[6] B. Hernández and E. Giraldo, A review of path planning and control for autonomous robots, *2018 IEEE 2nd Colombian Conference on Robotics and Automation (CCRA)*, pp.1-6, 2018.

[7] M. Guerra, D. Efimov, G. Zheng and W. Perruquetti, Avoiding local minima in the potential field method using input-to-state stability, *Control Engineering Practice*, vol.55, pp.174-184, 2016.

[8] T. Weerakoon, K. Ishii and A. A. F. Nassiraei, An artificial potential field based mobile robot navigation method to prevent from deadlock, *Journal of Artificial Intelligence and Soft Computing Research*, vol.5, no.3, pp.189-203, 2015.

[9] H. Y. Zhang, W. M. Lin and A. X. Chen, Path planning for the mobile robot: A review, *Symmetry*, vol.10, no.10, pp.450-466, 2018.

[10] X. Fan, Y. Guo, H. Liu, B. Wei and W. Lyu, Improved artificial potential field method applied for AUV path planning, *Mathematical Problems in Engineering*, pp.1-21, 2020.

[11] O. Khatib, Real-time obstacle avoidance for manipulators and mobile robots, *Proc. of 1985 IEEE International Conference on Robotics and Automation*, pp.500-505, 1985.

[12] S. S. Ge and Y. J. Cui, New potential functions for mobile robot path planning, *IEEE Transactions on Robotics and Automation*, vol.16, no.5, pp.615-620, 2000.

[13] J. Lee, Y. Nam and S. Hong, Random force based algorithm for local minima escape of potential field method, *2010 11th International Conference on Control Automation Robotics Vision*, pp.827-832, 2010.

[14] J. Choi, A potential field and bug compound navigation algorithm for nonholonomic wheeled robots, *2012 1st International Conference on Innovative Engineering Systems*, pp.166-171, 2012.

[15] C. Chen, T. Liu and J. Chou, A novel crowding genetic algorithm and its applications to manufacturing robots, *IEEE Transactions on Industrial Informatics*, vol.10, no.3, pp.1705-1716, 2014.

[16] T. D. Chen and Y. Y. Huang, Non-trap artificial potential field based on virtual obstacle, *2019 IEEE 16th International Conference on Networking, Sensing and Control (ICNSC)*, pp.275-280, 2019.

[17] P. Wang, S. Gao, L. Li, B. Sun and S. Cheng, Obstacle avoidance path planning design for autonomous driving vehicles based on an improved artificial potential field algorithm, *Energies*, vol.12, no.12, 2019.

[18] J. Sun, J. Tang and S. Lao, Collision avoidance for cooperative UAVs with optimized artificial potential field algorithm, *IEEE Access*, vol.5, pp.18382-18390, 2017.

[19] P. Sudhakara, V. Ganapathy, B. Priyadharshini and K. Sundaran, Obstacle avoidance and navigation planning of a wheeled mobile robot using amended artificial potential field method, *Procedia Computer Science*, vol.133, pp.998-1004, 2018.

[20] S. M. H. Rostami, A. Kumar, J. Wang and X. Liu, Obstacle avoidance of mobile robots using modified artificial potential field algorithm, *EURASIP Journal on Wireless Communications and Networking*, vol.70, pp.1-19, 2019.

[21] D. Wang, C. Li, N. Guo, Y. Song, T. Gao and G. Liu, Local path planning of mobile robot based on artificial potential field, *Proc. of the 39th Chinese Control Conference*, pp.3677-3682, 2020.

[22] X. Jiang and Y. Deng, UAV track planning of electric tower pole inspection based on improved artificial potential field method, *Journal of Applied Science and Engineering*, vol.24, pp.123-132, 2021.

[23] H. Ahmad, A. N. F. M. Pajeri, N. A. Othman, M. M. Saari and M. S. Ramli, Analysis of mobile robot path planning with artificial potential fields, *Proc. of the 10th National Technical Seminar on Underwater System Technology*, Singapore, pp.181-196, 2019.